Results in Engineering 28 (2025) 108233

Contents lists available at ScienceDirect

Results in Engineering

journal homepage: www.sciencedirect.com/journal/results-in-engineering

Research paper

Toward the sustainable stabilization of dredged sediment using biopolymers: a mechanical performance study

Yaser Ghafoori [a,*], Pooria Ghadir [b], Sabina Dolenec [c,d], Stanislav Lenart [e]

[a] Department of Geotechnics and Traffic Infrastructure, Slovenian National Building and Civil Engineering Institute, Dimičeva ulica 12, 1000 Ljubljana, Slovenia
[b] Visiting researcher, Slovenian National Building and Civil Engineering Institute, Dimičeva ulica 12, 1000 Ljubljana, Slovenia
[c] Department of Materials, Slovenian National Building and Civil Engineering Institute, Dimičeva ulica 12, 1000 Ljubljana, Slovenia
[d] Department of Geology, Faculty of Natural Sciences and Engineering, University of Ljubljana, Aškerčeva cesta 12, 1000 Ljubljana, Slovenia
[e] Department of Geotechnics and Traffic Infrastructure, Slovenian Building and Civil Engineering Institute, Dimičeva ulica 12, 1000 Ljubljana, Slovenia

ARTICLE INFO

Keywords:
Dredged sediment
Biopolymer
Stabilization
Mechanical characterization

ABSTRACT

Each year, over one billion cubic meters of sediments are dredged from ports and inland water bodies to maintain navigability and ensure infrastructure safety, creating significant landfill and environmental challenges. Dredged sediments are typically characterized by high moisture content, low bearing capacity, and limited shear strength. Their sustainable reuse requires effective stabilization and remediation strategies. Recent advancements in soil stabilization have increasingly focused on sustainable bio-binders, particularly biopolymers, due to their eco-friendly properties. This study evaluates the effectiveness of four biopolymers, namely calcium alginate (AL), chitosan (CH), xanthan gum (XA), and guar gum (GG) as sustainable bio-binders for improving dredged sediments from the Port of Koper, Slovenia. Mechanical testing demonstrated that 1 wt% XA, AL, and CH increased unconfined compressive strength by 40 %, 29 %, and 10 %, respectively. Direct shear tests revealed that AL and XA increased cohesion by 52 % and 104 %, respectively, while reducing the friction angle by 4° In contrast, CH and GG enhanced both cohesion (by 81 % and 37 %, respectively) and the friction angle (by 1° in each case). Consolidation characteristics were also improved, with reduced settlement under normal load. Microstructural analysis identified the formation of biopolymer matrices including fibrous networks, gel films, and particle clusters that explain the mechanical improvements. The findings confirm that biopolymer stabilization is a viable technique to convert dredged marine sediments into engineered materials, minimizing landfill disposal, and supporting the transition to more sustainable construction practices.

1. Introduction

Dredged sediments (DS) are predominantly composed of fine-grained silts and clays [1], which are typically generated from port and harbor areas, as well as from inland water bodies such as rivers, lakes, and reservoirs. Excessive sediment accumulation poses persistent challenges for coastal, offshore, and inland water engineering, necessitating frequent dredging operations to maintain navigability, storage capacity, and structural safety. Globally, more than one billion cubic meters of sediment are dredged each year [2], with annual volumes ranging from 200 to 500 million cubic meters in the United States [3] and around 300 million tons in Europe [4]. At present, most dredged sediments are managed as waste and disposed of either at sea or in landfills [5]. Such practices generate serious environmental impacts while rapidly consuming the limited disposal capacity. Reusing dredged sediments in construction therefore offers a sustainable solution to reduce disposal pressures and conserve natural resources.

However, DS typically exhibit high moisture content, low shear and compressive strength, and they are often contaminated with heavy metals and microplastics [6]. With water contents often exceeding 100 % of dry weight and undrained shear strengths below 25 kPa [7], these materials are prone to excessive settlement and instability, underscoring the need for sustainable stabilization strategies. Conventional binders such as cement, lime, and fly ash can improve strength [8,9] but carry substantial environmental burdens due to CO_2 emissions and potential heavy metal leaching [10–12]. These environmental concerns have

* Corresponding author.
E-mail addresses: yaser.ghafoori@zag.si (Y. Ghafoori), pooria_ghadir@yahoo.com (P. Ghadir), sabina.dolenec@zag.si (S. Dolenec), stanislav.lenart@zag.si (S. Lenart).

https://doi.org/10.1016/j.rineng.2025.108233
Received 24 October 2025; Received in revised form 13 November 2025; Accepted 14 November 2025
Available online 17 November 2025

encouraged the search for low-carbon alternatives that balance environmental integrity with engineering performance.

Several studies have been conducted to develop environmentally friendly techniques for improving the mechanical properties of weak soils to enable their application as construction materials. Among these, the microbial geotechnical method, which utilizes microorganisms for bioclogging and biocementation, has been explored to enhance DS behavior. In this process, biocementation occurs through the microbially induced precipitation of calcium carbonate, which binds soil particles, reduces pore spaces, fills voids, and increases flocculation and density [13,14]. Wani and Mir [15] investigated the biocementation of dredged sediment and reported over a 300 % increase in unconfined compressive strength (UCS), along with significant improvements in both cohesion and friction angle of the treated material. In addition to biological approaches, other innovative solutions have focused on reusing waste materials for soil stabilization, such as the use of geothermally derived silica grout for soil improvement [16] and waste rubber tire powders mixed with cement for dredged sediment stabilization [17].

The present study investigates the use of biopolymers as natural and environmentally friendly binders to improve the mechanical properties of dredged sediments. Derived from renewable sources, biopolymers are biodegradable, typically non-toxic materials [18], and effective even at low dosages, making them promising candidates for sustainable soil stabilization. Biopolymer interactions, including gel formation, hydrogen bonding, ionic crosslinking, and flocculation [19], have been shown to enhance cohesion, reduce permeability [20], limit shrink-swell behavior [21], and improve durability [22] of soils without the environmental footprint of cementitious binders.

Xanthan gum (XA), a widely studied biopolymer produced by *Xanthomonas campestris* bacteria [23], has shown significant potential in soil stabilization. Studies on silt treated with 2 % XA under wetting cycles revealed notable increases in cohesion and friction angle at water contents below 10 %, though effects diminished at higher moisture content [24]. Investigations on clayey sand [25] and clayey silt-sand with both deionized and brine water [26] showed increased liquid limit and plasticity index, attributed to hydrogel formation and cross-linking within soil pores. Abbasi et al. [27] reported a significant increase in UCS for clayey sand treated with 0.25 % XA (by dry soil weight) after seven days of curing, supported by ultrasonic velocity measurements, which indicated improved stiffness and internal structure. Ren et al. [23] investigated the stabilization of weak soil using a combination of XA (hydrophilic biopolymer) and casein, a hydrophobic biopolymer. They reported that UCS and water resistance were significantly improved compared to both untreated samples and soils treated with XA or casein alone. Additionally, Lee et al. [22] found that blending XA with starch enhanced the durability of poorly graded sand under cyclic wetting-drying and freeze-thaw conditions.

Chitosan (CH), a cationic polysaccharide derived from chitin, has also shown strong potential for soil stabilization. Wang et al. [28] investigated the mechanical properties of sand and kaolinite clay using various CH contents and identified optimal dosages of 1.5 % (by weight of dry soil) for sand and 2 % for kaolinite. Their results highlighted the rapid development of strength within the first seven days of curing. They also found that a 0.5 % acetic acid solution was optimal for dissolving chitosan and achieving maximum strength gains in both sand and kaolinite. Several studies have demonstrated CH's effectiveness in sandy soils. Shariatmadari et al. [29] and Amiri Tasuji et al. [30] reported a significant increase in UCS with 0.32 % CH under dry curing conditions. Treated sand also showed improved resistance to wind erosion and a 35 % reduction in permeability [30]. In organic silt, UCS increased with CH content up to 2.5 %, with a 103 % gain at 28 days of curing, beyond which strength declined [31]. Similar results were observed in clayey soils, where a 1.5 % CH dosage yielded a 104 % UCS improvement after 28 days [32]. Hataf et al. [33] found that CH improved UCS by approximately 50 % and reduced hydraulic conductivity in fine-grained soils. These improvements were attributed to the formation of polymeric bridges between clay particles, as confirmed by microstructural analysis, which revealed enhanced cohesion and interparticle connectivity.

Guar gum (GG), derived from the endosperm of *Cyamopsis tetragonoloba*, has shown promise in stabilizing loess soils. Rong et al. [34] reported that 2 % GG (by weight of dry soil) significantly reduced disintegration and increased UCS, cohesion (by 44.0 %), and internal friction angle (by 12.5 %) after 14 days of curing. Du et al. [35] further observed improvements in water retention, reduced soil degradation, and enhanced shear strength. However, repeated wet–dry cycles reduced cohesion, friction angle, and water retention capacity in treated loess, highlighting the need to consider durability in long-term applications.

Calcium alginate (AL), a calcium salt of alginic acid extracted from brown seaweed, has mainly been investigated for its role in reducing contaminant leaching from polluted soils [36,37]. Its ionic crosslinking capability, often referred to as the "egg-box" structure [38], is thought to facilitate mechanical bonding and improve durability. While sodium alginate has been studied more extensively for soil stabilization [39,40], the application of calcium alginate in this field remains limited and calls for further exploration.

Despite increasing evidence of biopolymer effectiveness in soft soils and sands, their role in dredged sediment stabilization remains underexplored. Existing studies are fragmented and often focus on single polymers, leaving uncertainty about comparative performance across different biopolymer types. Moreover, while XA, CH, and GG have been studied to some extent, AL has received little attention in soil stabilization contexts.

To address these gaps, this study investigates the stabilization of dredged sediments from the Port of Koper, Slovenia, using four biopolymers. Atterberg limits were assessed at 0.5 %, 1.0 %, and 2.0 % weight ratios, while mechanical performance at 1 wt % was examined through UCS, direct shear, cone penetration, and volumetric shrinkage tests. SEM/EDS analyses were performed to investigate polymer-soil interactions. Rather than identifying an optimal dosage, this study provides a comparative framework for evaluating the performance of biopolymer in dredged sediment stabilization, focusing on marine sediments from the Port of Koper.

2. Methodology

2.1. Material

The sediment utilized in this study was dredged from the Port of Koper, Slovenia (45° 33′ 47″ N, 13° 44′ 19″ E). Its mineralogical composition was previously characterized by Šmuc et al. (2018) [41] by quantitative X-ray diffraction (QXRD) of 21 samples, which identified quartz, calcite, and illite as the predominant mineral phases with smaller amounts of albite and dolomite. The grain size of sediment was determined by the sedimentation analysis method implemented in the hydrometer according to ISO 17892–4:2016 [42]. The sediment comprises approximately 33 % clay and 67 % silt. To evaluate its compaction characteristics, a standard Proctor test [43] was performed, and values for the optimum moisture content (OMC) and the maximum dry density (MDD) were determined. The fundamental geotechnical properties of the sediment are summarized in Table 1, while the grain size distribution and Proctor test results are illustrated in Fig. 1.

Four widely used and commercially available biopolymers were selected in this study. Calcium Alginate (AL, product number A0738) and Xanthan Gum (XA, product number X0048) were obtained from Tokyo Chemical Industry Co., Ltd. (TCI). Chitosan (CH, product no 417963), derived from shrimp harvested in Iceland, and Guar Gum (GG, product no G4129) were both obtained from Sigma-Aldrich (Merck).

2.2. Sample preparation

Dredged sediment was washed, sieved through a 1 mm sieve mesh,

Table 1
Results of dredged sediment characterization.

Natural water content	Specific gravity (G_s)	Liquid limit (LL)	Plasticity index (PI)	Unified soil classification (USCS)	Optimum moisture content (OMC)	Maximum dry density (MDD)
47 %	2.7	58 %	37	High-plasticity clay (CH)	17.8 %	1.75 g/cm^3

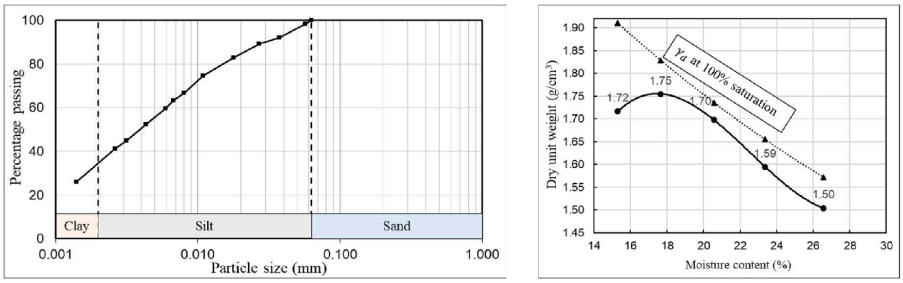

(a) (b)

Fig. 1. (a) Grain size distribution of dredged sediment; (b) Proctor compaction test.

and oven-dried at 50 °C to remove moisture while preserving its natural mineralogy and organic content. Standard drying at 105 °C can alter clay minerals and degrade organics. Drying at 50 °C maintained the sediment's chemical integrity and pore structure, ensuring realistic behavior in subsequent stabilization and mechanical tests.

Biopolymer gels were prepared by dissolving each biopolymer in distilled water at prescribed concentrations. For AL and GG, the biopolymers were directly added to water maintained at 23 ± 0.2 °C. Both dissolved effectively at this ambient temperature. In the case of XA, the water was preheated to 50 °C using a stirring heater, after which the biopolymer was gradually introduced. The solution was stirred continuously for over 30 min to form a homogeneous gel and was subsequently cooled to the reference temperature of 23 °C. To dissolve CH, a 2 % (by weight of water) acetic acid solution was first prepared, into which the biopolymer was slowly added. The mixture was stirred for over 30 min using magnetic stirring to achieve a homogeneous gel. The resulting biopolymer gels were then combined with the dried sediment and manually mixed using a spatula to produce a uniform composite. The sample preparation procedure is illustrated in Fig. 2.

2.3. Experimental studies

Initially, the Atterberg limits of the biopolymer-treated sediment were obtained with the three concentrations of biopolymer associated with 0.5 %, 1 %, and 2 % of the weight of the dry sediment. The liquid limit (LL) was determined by the fall cone test using a standard cone with 80 g mass and a 30° tip angle. In accordance with ISO 17892–12:2018 [44], the liquid limit is defined as the water content at which the cone penetrates 20 mm into the soil. To determine this, water content was incrementally increased, and cone penetration was measured at a minimum of four different moisture levels. The plastic limit (PL) of the specimens was also determined following the same ISO standard. The consistency of the treated sediment was subsequently evaluated by calculating the consistency index based on the Atterberg limit results. Based on these findings, the 1 wt % biopolymer concentration was selected for further investigation, as it provided a representative response across the range of treatments.

The fall cone method was also employed to estimate the undrained shear strength of the treated sediment based on the empirical correlation developed by Hansbo [45] and in accordance with the procedures outlined in EN ISO 17892–6:2017 [46].

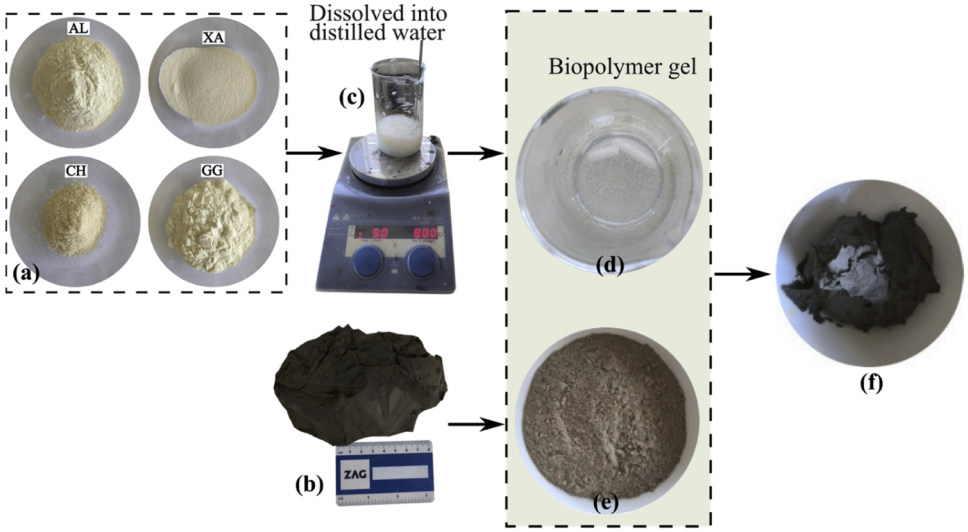

Fig. 2. a) Four biopolymer (AL, XA, CH, GG) powders, b) Dredged sediment at natural condition, c) Dissolving biopolymer powder in distilled water, d) Formation of biopolymer gel, e) Dried sediment, and f) Sediment-biopolymer homogenous mixture.

$$C_u = c.g.\frac{m}{i^2} \quad (1)$$

where C_u is the undrained shear strength [kPa], c is a dimensionless constant that depends on the cone tip angle (taken as 0.8 for a 30° tip), g is the gravity acceleration, m is the mass of the cone [g], and i is the average penetration depth of the cone [mm].

Shrinkage behavior and the rate of water loss in the sediment were investigated by preparing soil samples with a water content of 58 %, corresponding to the liquid limit of the untreated dredged sediment. The moist sediment was placed into the cylindrical glass molds with a diameter of 47 mm and a height of 23 mm. The samples were allowed to dry under controlled laboratory conditions for over 10 days at a stable temperature of 20±0.2 °C and relative humidity of 80±3 3 %. Surface shrinkage was monitored via image processing, with images captured at regular time intervals. Volumetric shrinkage was assessed using the paraffin-coated immersion method [47] after the samples were fully dried. Concurrently, the rate of water loss was determined by recording the weight of the samples at fixed time intervals during the drying process.

The unconfined compressive strength (UCS) of both untreated and biopolymer-treated sediment was determined in accordance with ISO 17892–7:2017 [48]. Soil specimens were manually compacted in three layers into cylindrical molds with a diameter of 36 mm and a height of 78 mm, at a water content of 17.8 %, corresponding to the OMC of the untreated sediment. A dry density of 1.56 ± 0.03 g/cm^3 was achieved for the untreated samples as well as those treated with AL and XA biopolymers. In contrast, samples treated with CH and GG reached a slightly lower dry density of 1.50 ± 0.02 g/cm^3. For each material, three specimens were prepared and cured for 28 days. During the curing period, the samples were wrapped in plastic and stored in an incubator to maintain humidity. UCS tests were conducted using a strain-controlled apparatus, with the strain rate set at 0.6 mm/min.

Specimens for the direct shear test were prepared by incorporating 1 wt % biopolymer and molding the mixture into square plate samples with dimensions of 23 mm in height and 60 × 60 mm in surface area. The samples were compacted at a water content of 17.8 % to achieve a target dry density of 1.68 ± 0.02 g/cm^3. After compaction, the specimens were wrapped in plastic and cured for 28 days in a laboratory incubator under controlled conditions. The direct shear tests were performed using a digital direct shear apparatus [49] and in accordance with the procedures outlined in ISO 17892–10:2019 [50]. Shear tests were conducted under three normal stress levels (50 kPa, 100 kPa, and 200 kPa) using a constant shear displacement rate of 0.01 mm/min. Prior to shearing, the specimens were allowed to consolidate under their respective normal stresses for 24 h.

The microstructure of the soil specimens was examined using Scanning Electron Microscopy (SEM) to investigate the interaction between sediment particles and biopolymers. Microstructural observations were performed with a JEOL IT500 LV SEM, which operated at an accelerating voltage of 20 kV in low vacuum mode and a working distance of 10 mm. Fine specimens were taken from failed UCS samples, which were aged for 120 days. To complement the morphological observations, Energy-Dispersive X-ray Spectroscopy (EDS) was performed to identify and quantify the elemental composition of the treated soil.

3. Results

3.1. Consistency

The liquid and plastic limits of the untreated sediment, as well as those treated with 0.5, 1, and 2 wt % biopolymer were determined as presented in Fig. 3.

With the exception of AL, all tested biopolymers significantly increased the liquid limit of the sediment. Regarding the plastic limit, CH was the only biopolymer that led to a notable increase. Even at a concentration of 2 wt %, AL showed no effect on either the LL or PL of the sediment. For the specimen treated with 2 wt % CH, the plastic limit could not be determined, as the mixture formed a dispersed paste that did not exhibit the characteristic plastic behavior during rolling.

The observed increase in LL for most biopolymers can be attributed to hydrogel formation, enhanced particle bonding, increased fluid viscosity, and pore space obstruction. All four biopolymers used in this study are hydrophilic [51], allowing them to absorb water and form viscous hydrogels that immobilize water molecules, thereby elevating the LL. The lack of LL increase in AL-treated samples may be associated with inadequate curing time, as AL typically requires sufficient curing to develop a water-retentive hydrogel matrix capable of influencing soil consistency [52].

To evaluate the relative stiffness and consistency state of the treated sediment, the consistency index was calculated based on the measured natural water content of 47 %. Using the LL and PL values shown in Fig. 3, the resulting consistency indices are presented in Fig. 4.

As illustrated in the figure, the consistency index of the sediment increases significantly with the addition of biopolymers, even at concentrations as low as 0.5 wt %, with the exception of AL. The results clearly indicate distinct differences in the firmness of the treated samples. Among the treatments, CH and GG exhibited the most pronounced effect with the highest consistency indices. Notably, at a biopolymer concentration of 1 wt %, both CH and GG enhanced the consistency index by approximately 100 %, which highlights their effectiveness in

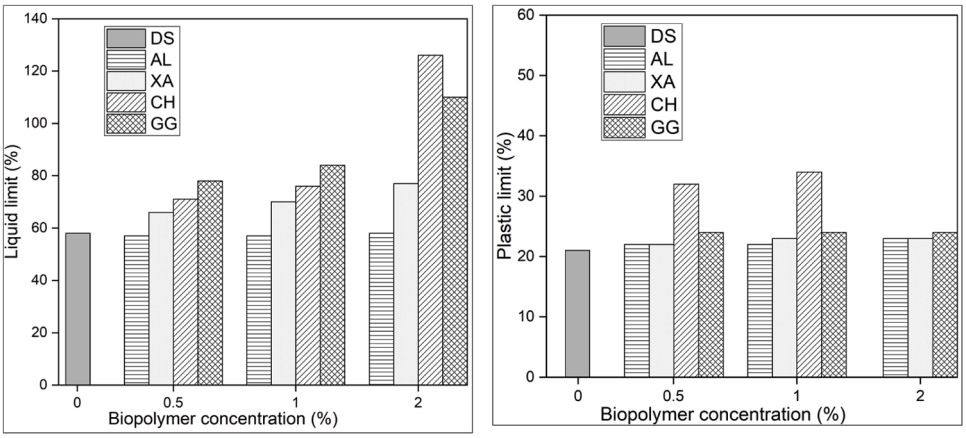

Fig. 3. Atterberg limits of sediment treated by biopolymers; a) Liquid limit, b) Plastic limit.

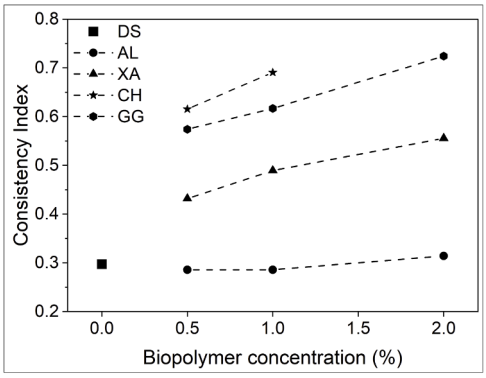

Fig. 4. Consistency index of treated sediment with 0.5, 1, and 2 % weight ratio biopolymers.

improving the structural firmness of the sediment. These findings suggest that CH- and GG-treated samples transition into a firmer, semi-solid state at an early age, whereas AL-treated specimens remain comparatively softer and more prone to deformation.

Based on the results of the Atterberg limit tests, a biopolymer concentration of 1 % by dry sediment weight was selected for subsequent investigations. The moisture retention behavior of the samples under laboratory drying condition is expressed in terms of water loss over time in Fig. 5. As shown, with the exception of CH, the effect of 1 wt % biopolymer concentration on the evaporation rate is minimal. The CH-treated sample exhibited a noticeably slower drying rate, which can be attributed to its ability to block pore spaces [28] and the inherent water retention capacity of CH hydrogel [33]. These properties hinder moisture evaporation and consequently prolong the drying process.

Volumetric and surface shrinkage tests were conducted to assess the shrink-swell potential of the sediment during drying. The results are illustrated in Fig. 6, which presents the surface and volumetric shrinkage behavior of the samples.

As observed, the addition of 1 wt % biopolymer reduces the susceptibility of the soil to shrinkage. During the drying process, capillary suction (negative pore pressure) develops as water evaporates from the sample surface. This suction draws soil particles closer together, reduces void spaces, and leads to a rearrangement of particles within the soil matrix, ultimately resulting in shrinkage. Biopolymers mitigate this effect by forming a cohesive network within the pore spaces, effectively reducing the void ratio up to an optimal concentration. However, beyond this optimal dosage, further biopolymer addition may lead to an increase in void ratio due to the formation of excessive gel structures or flocculation effects [53].

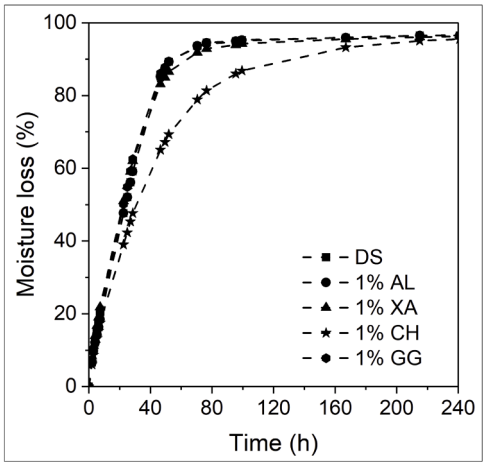

Fig. 5. Water loss rate for untreated sediment and biopolymer-treated sediment.

Both surface and volumetric shrinkage were found to decrease with the addition of biopolymers, as illustrated in the results. This reduction is evident across all treated samples, with particularly pronounced effects observed in those treated with XA and CH. It is also worth noting that during the shrinkage tests, no surface cracking was observed in either the treated or untreated samples with the exception of the AL-treated specimen, where one visible crack was detected.

3.2. Mechanical characterization

The cone penetration test was used to estimate the undrained shear strength (C_u) of the samples in their fresh state, immediately following the preparation of the biopolymer-sediment mixtures. Measurements were conducted at varying water contents for specimens treated with 1 wt % biopolymer concentration. The resulting data are presented in Fig. 7.

A clear inverse relationship was observed between water content and C_u, with the undrained shear strength decreasing as water content increased. All biopolymer-treated samples exhibited significantly higher C_u values compared to the untreated sediment with CH and GG showing the most substantial improvements. Notably, for biopolymer-treated specimens, C_u increased exponentially at lower water contents. The results indicate that treated DS gain shear strength immediately after mixing, before any curing takes place. This early strength gain is critical in geotechnical applications where initial load-bearing capacity and structural integrity are essential during handling, placement, or early construction phases.

The UCS of the samples was determined after 28 days of curing. Even at a concentration of 1 wt %, biopolymer addition significantly improved the compressive strength of the sediment. The UCS stress-strain curves for the untreated DS and the biopolymer-treated samples are shown in Fig. 8. Each curve reveals characteristic behaviors such as stiffness, peak strength, ductility, and post-failure deformation patterns.

The pre-failure behavior of the specimen was assessed by calculating the secant modulus of sediment (E_{50}) defined as the slope to a point on the stress-strain curve where the stress is 50 % of the peak stress. The secant modulus represents the initial stiffness of the soil specimen and its resistance to deformation. As presented in Table 2, AL-treated sediment displayed the highest initial stiffness, reaching a stress value exceeding 280 kPa at just 0.65 % strain.

Samples treated with XA and CH also demonstrate a good initial stiffness enhancement, although their deformation behavior differs from AL-treated sediment. They demonstrate more moderate stiffness, which develops stress gradually over longer strain intervals and implies more ductile material behavior in the pre-failure stage. In contrast, untreated sediment and the GG-treated sediment show low secant modulus, which means they deform more easily under compressive stress. XA and AL treated sediment also show a longer and clearer linear elastic phase followed by a more gradual transition into nonlinear plastic yielding before peak.

In terms of peak compressive strength, the XA-treated sediment exhibited the highest performance, which reached a maximum stress of 621 kPa and a failure strain of 3.3 %. Xanthan gum significantly improved both the load-bearing capacity and ductility of DS. The AL-treated sample achieved a peak strength of 572 kPa, but the failure strain remained the same as the untreated sample at 2.8 %, indicating that alginate did not enhance the ductility of the sediment under normal compressive stress. The CH-treated sample also showed strong performance with slightly lower peak strength and moderate ductility. In contrast, the GG-treated sample fails at a lower stress and at a similar strain to the untreated sediment. It should be noted that all samples were prepared using the optimum moisture content (OMC) of the untreated sediment. Preparing the samples at the respective OMC specific to each biopolymer-treated sediment would result in a more pronounced enhancement of compressive strength.

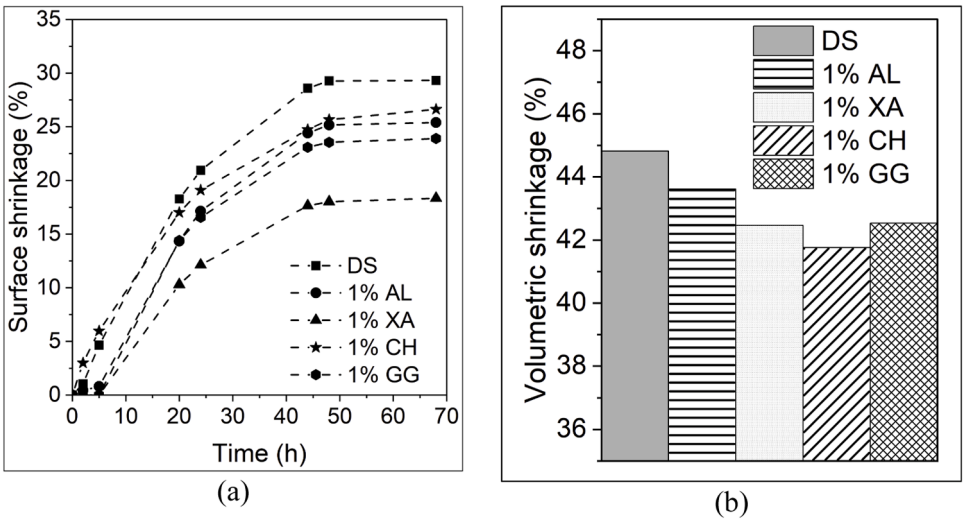

Fig. 6. (a) Surface shrinkage of sediment samples; (b) Volumetric shrinkage.

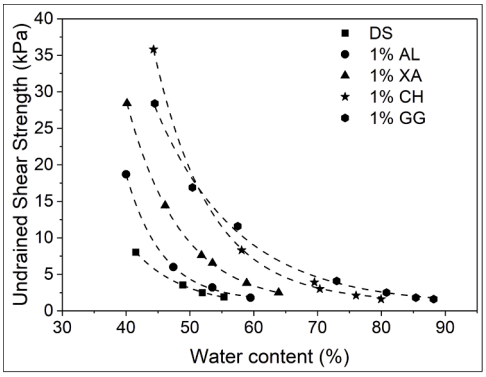

Fig. 7. Estimated undrained shear strength by the cone penetration test.

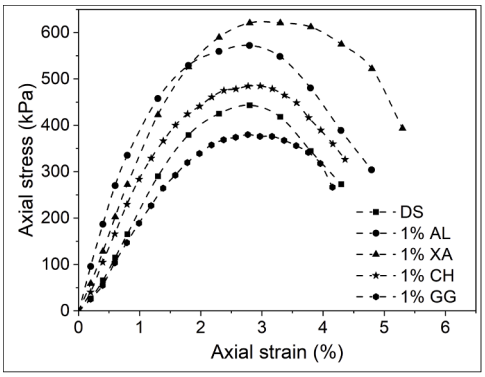

Fig. 8. Stress-strain behavior under UCS test.

Table 2
Compressive strength, failure strain, and secant modulus of sediment samples.

Specimen	DS	1 % AL	1 % XA	1 % CH	1 % GG
Compressive strength (kPa)	443	572	621	485	380
Failure strain (%)	2.8	2.8	3.3	3.0	2.9
Secant modulus, E_{50} (MPa)	21.6	44.1	33.5	28.9	19.1
Strain of E_{50} (%)	1.02	0.65	0.93	0.84	1.00

Biopolymer addition (except in the case of GG) also slightly enhanced the post-failure ductility of the sediment. While the untreated sample exhibited brittle behavior with an abrupt drop in stress after reaching peak strength, the AL- and XA-treated specimens demonstrated a more gradual stress decline.

The failure morphology of the treated and untreated DS samples was visually assessed during loading at the onset of failure and in the post-failure phase, as illustrated in Fig. 9. The observed failure patterns revealed distinct differences between treated and untreated specimens in terms of crack initiation and failure mechanisms.

The GG-treated sediment failed predominantly through a shear mechanism, characterized by the formation of a well-defined diagonal crack that developed into an inclined shear failure plane. In contrast, the AL-treated sample exhibited tensile failure with prominent vertical splitting caused by longitudinal cracks parallel to the direction of loading. Similarly, the CH-treated specimen also failed primarily through tensile action. A noticeable horizontal failure plane emerged that divided the sample into upper and lower segments. This failure pattern may suggest weaker interlayer bonding in the CH-treated soil, potentially due to the manner in which the biopolymer gel is distributed within the matrix.

For the untreated sediment and the XA-treated sample, a more complex failure morphology was observed. The crack patterns indicated a combination of shear and tensile features, which implies a mixed-mode failure mechanism. This suggests that the failure was governed by the interaction of both shear and tensile strength limitations within the sediment matrix.

Direct shear tests were performed on samples compacted at the optimum moisture content of the untreated sediment and cured for 28 days. Prior to testing, the specimens were saturated and allowed to consolidate for 24 h to simulate field-like conditions. This allowed us to evaluate the settlement behavior of the samples under three different normal stress levels, as demonstrated in Fig. 10. In all cases the curves present a steep initial slope, indicating the immediate compression upon load application. The untreated sediment showed the greatest settlement, which increased with the applied stress as expected. Under a normal load of 200 kPa, the saturated untreated sediment settled approximately 0.8 mm, which shows relatively high compressibility and limited resistance to volumetric deformation. In contrast, the addition of AL and CH biopolymers markedly reduced settlement across all applied normal stress levels. These biopolymers significantly enhanced the stiffness of the sediment at saturation condition and reduced its compressibility. The XA-treated sample displayed intermediate performance, as it effectively reduced settlement compared to the untreated

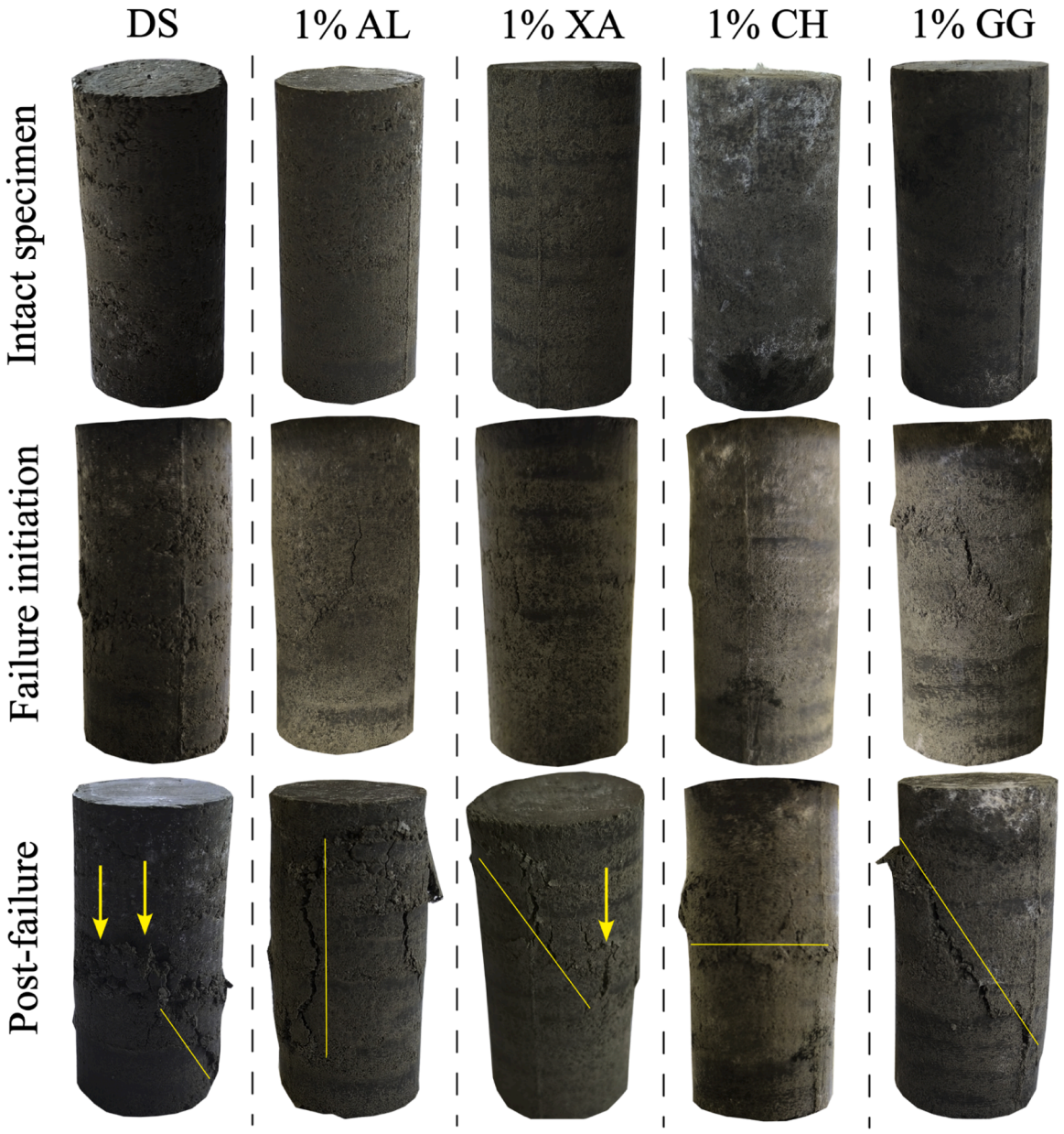

Fig. 9. The failure morphology of untreated and biopolymer-treated samples under the UCS test.

sediment but to a lesser extent than the AL and CH-treated samples. Unlike the other biopolymers, GG did not reduce the compressibility of the sediment. Its performance was comparable to that of the untreated sample.

The results of direct shear tests in terms of shear stress versus shear strain curves are presented in Fig. 11. The results indicate that all specimens exhibit strain-softening behavior, which is characterized by a distinct peak shear strength followed by a gradual reduction in shear stress and eventually approaching a residual or stable value. Such a pattern was also observed in the study by Gu et al. [54], where silty clay soil treated with XA at water contents of 5 % and 15 % demonstrated the same trend as in the present work. In their study, the treated fine soil reached peak shear stress at 3–4 % strain, after which the stress gradually dropped and remained constant at a residual level higher than that of the untreated soil. In addition to the type and dosage of the additive, the strain behavior of treated soils also depends strongly on the soil type. A study by Soldo and Miletić [55] reported that clay soil treated with 1 wt % XA exhibited a more ductile response, with only a minor reduction in shear stress after the peak, while sand treated with the same dosage showed a distinctly brittle behavior, characterized by a sharp post-peak stress drop.

The addition of biopolymers resulted in an increase in peak shear strength for all treated samples. Among all treatments, the CH-treated sample exhibited the highest peak shear strength across all three applied normal stress levels. The XA-treated specimen also demonstrated enhanced post-peak behavior, with a more stable decline in shear stress and a clearly elevated residual strength compared to the untreated sample. Furthermore, the XA-treated sediment showed a significant improvement in ductility. The shear strain developed more gradually, and the strain at peak shear strength was the highest among all samples, which indicates a greater capacity for deformation before failure. These results suggest that XA not only improves strength but also contributes to a more ductile failure response.

The relationship between normal stress and shear stress for all samples is illustrated in Fig. 12. The corresponding values of cohesion and internal friction angle, derived from these plots, are summarized in Table 3. As observed, biopolymer treatment significantly increases the cohesion of the sediment primarily through physicochemical bonding

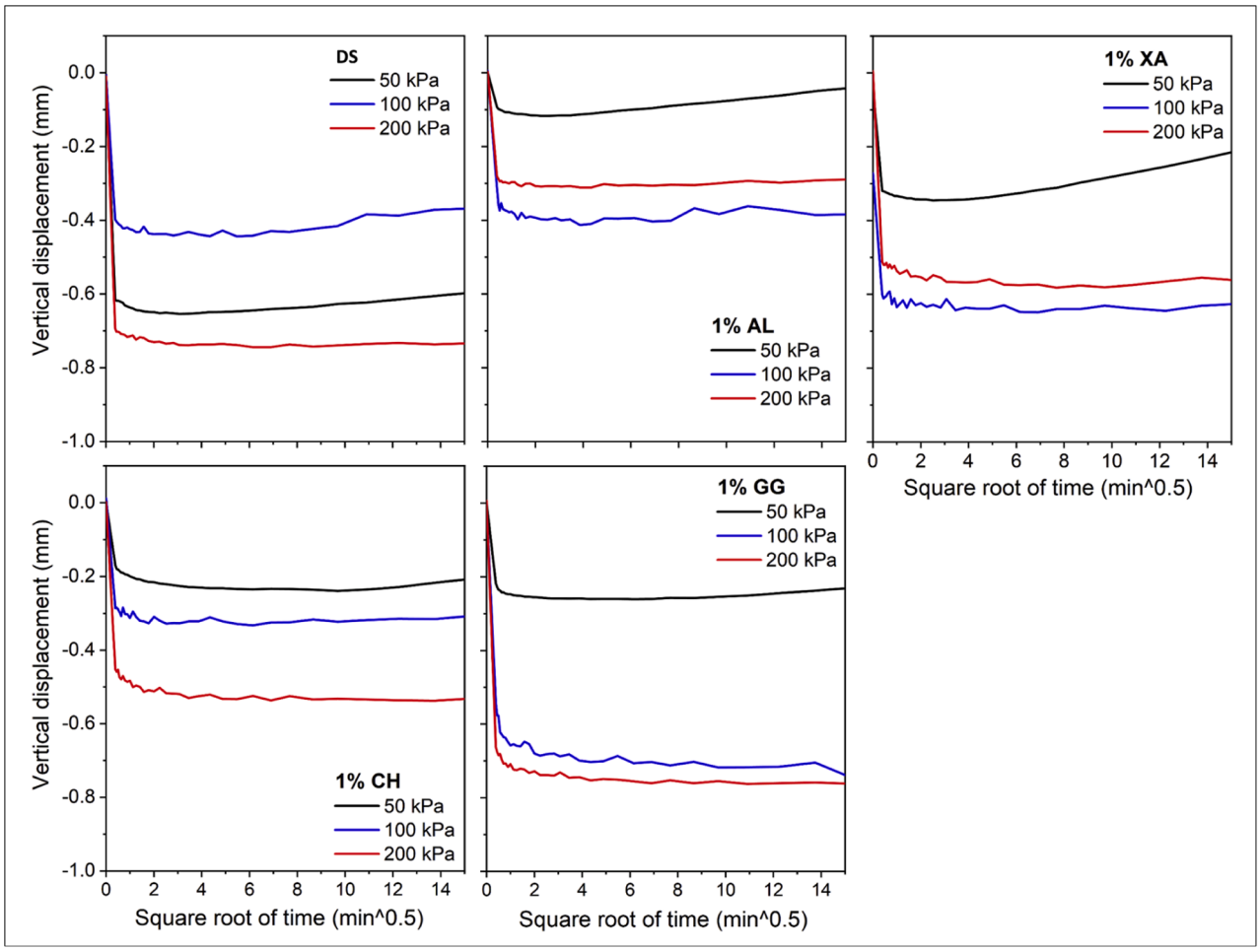

Fig. 10. Consolidation test for three normal stresses.

mechanisms. In contrast, the friction angle remains mainly unaffected or even decreases slightly, particularly in the cases of XA- and AL-treated samples. The increase in cohesion ranges from 37 % in the GG-treated specimen (the lowest among the treated samples) to a maximum of 103 % in the XA-treated sample. This enhancement is attributed to the formation of hydrogels, which create cohesive bonds between sediment particles and strengthen interparticle interactions. These gel networks improve the overall structural integrity of the sediment matrix and contribute to the shear strength development of biopolymer-treated samples.

Conversely, the friction angle is governed by factors such as particle shape, surface roughness, and resistance to interparticle sliding. Biopolymers do not significantly alter the grain shape or surface friction. In fact, the application of biopolymers may result in a thin film coating on particle surfaces, which can reduce interparticle friction by acting as a lubricating layer, thereby decreasing the sliding resistance and contributing to the observed reduction in friction angle for certain biopolymer-treated samples.

3.3. Microscopic analysis

Fig. 13 presents the SEM images and EDS spectra of sediment specimens treated with biopolymers. This figure depicts samples from the UCS test, compacted and prepared at an optimal water content of 17.8 %.

In the untreated sample (DS), the sediment particles appear loosely aggregated, exhibiting irregular surfaces with limited bonding between the grains. The EDS spectra (Spectra 1 and 2) show the presence of dominant elements such as oxygen (O), silicon (Si), aluminum (Al), and iron (Fe), which are consistent with clay mineral phases.

Upon the addition of AL, a clear microstructural effect was observed. AL partially coated the sediment particles, formed bridge-like connections between the adjacent aggregated particles, and filled the pore spaces. These biopolymer bridges were measured <1 μm in diameter. Elemental mapping through EDS showed increased carbon (C) concentrations in the AL-treated regions, confirming the presence of the organic biopolymer matrix alongside the mineral components of the soil.

In the sample treated with XA, distinct fibrous structures with elongated morphology were observed, some reaching widths of up to approximately 8.6 μm. These fibrous networks were seen wrapping around sediment particles, effectively binding them together and enhancing inter-particle adhesion. The EDS spectra from these zones displayed elevated peaks for C and O, confirming the presence of XA within the soil matrix.

The sample treated with CH exhibited bridge-shaped and cluster-like formations, with diameters typically under 2 μm, distributed across the sediment surface. These formations contributed to the development of a denser microstructure, effectively reducing pore spaces within the soil matrix. EDS spectra further confirmed the incorporation of CH, showing increased C and O peaks while still preserving the characteristic mineral signals of Si, Al, Fe, and magnesium (Mg).

In the case of the GG-treated sample, a continuous bridging network is evident, with biopolymer films spanning up to 60 μm across the particle surfaces. This extensive coverage enhances particle cohesion. EDS results confirm the organic origin of the biopolymer phase, indicated by a high proportion of C and O in addition to the typical soil

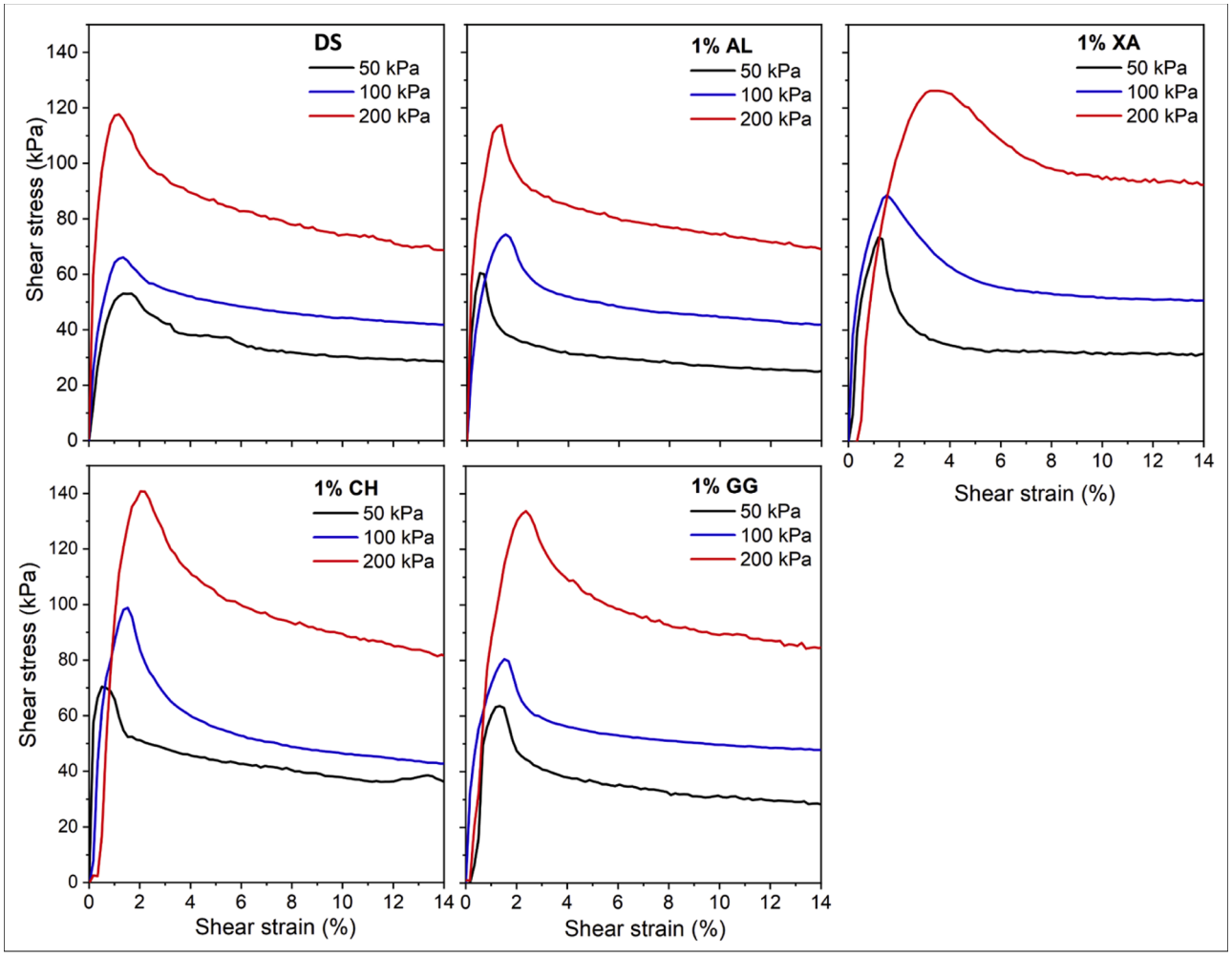

Fig. 11. Direct shear test results of untreated and biopolymer-treated samples.

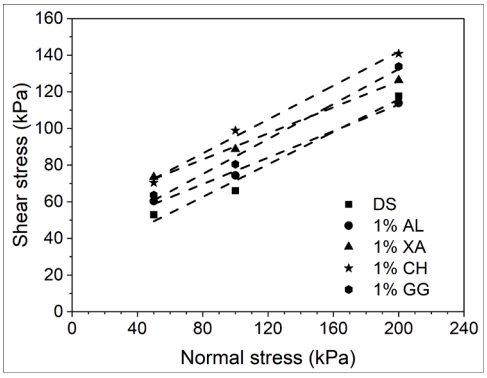

Fig. 12. Shear stress-normal stress.

Table 3
Shear strength characteristics of DS treated with biopolymers.

Specimen	DS	1 % AL	1 % XA	1 % CH	1 % GG
Cohesion (kPa)	27	41	55	49	37
Friction angle	24°	20°	20°	25°	25°

elements.

4. Discussion

A summary of the experimental results of this study is indicated in Fig. 14, comparing the effect of different biopolymers on improving the geotechnical properties of the dredged sediment. CH and GG biopolymers formed a highly viscous gel, which subsequently increased the liquid limit significantly >100 %. With the exception of AL, the consistency of the treated sediment increased significantly by treating with biopolymers. This enhancement is attributed to the formation of hydrogel between soil particles, which strengthens inter-particle bonds as observed in the SEM images. In contrast, the AL biopolymer required additional curing time to develop a water-retentive hydrogel [52]; consequently, early-age tests for LL, PL, and undrained shear strength showed no significant improvement.

Treatment of DS with biopolymers decreased the volumetric shrinkage slightly while it slightly increased the capability of water retention during the drying process. The CH-treated sample presented the slowest rate of drying during the shrinkage test.

In the case of compressive strength, XA- and AL-treated sediment exhibit sound enhancement in terms of peak strength and secant modulus at 28 days of curing. XA also increased the ductility of sediment, as axial strain at the failure during the UCS test was increased by 17 % compared to the untreated sample. The consolidation test showed that AL, XA, and CH biopolymers significantly decreased the settlement of saturated DS under normal loads.

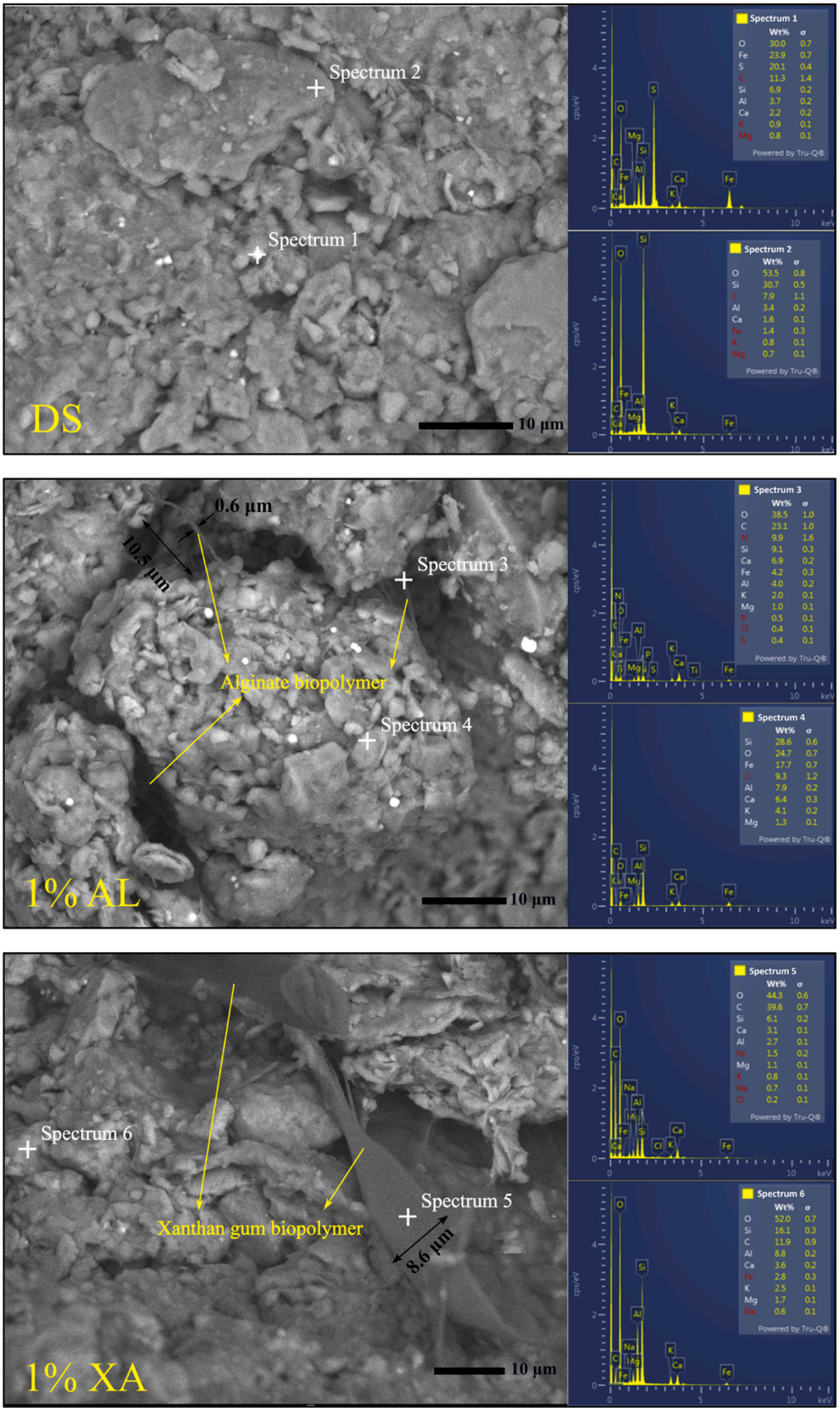

Fig. 13. SEM/BSE microphotographs and EDS spectra of sediment specimens extracted from the UCS samples.

In contrast to lime treatment, where cohesion tends to remain relatively stable and the friction angle increases with lime content [7], the effect of biopolymers is primarily observed in enhancing the cohesion of the sediment, with minimal or even negative influence on the friction angle. Among the tested biopolymers, XA produced the most significant increase in cohesion. However, this was accompanied by a notable

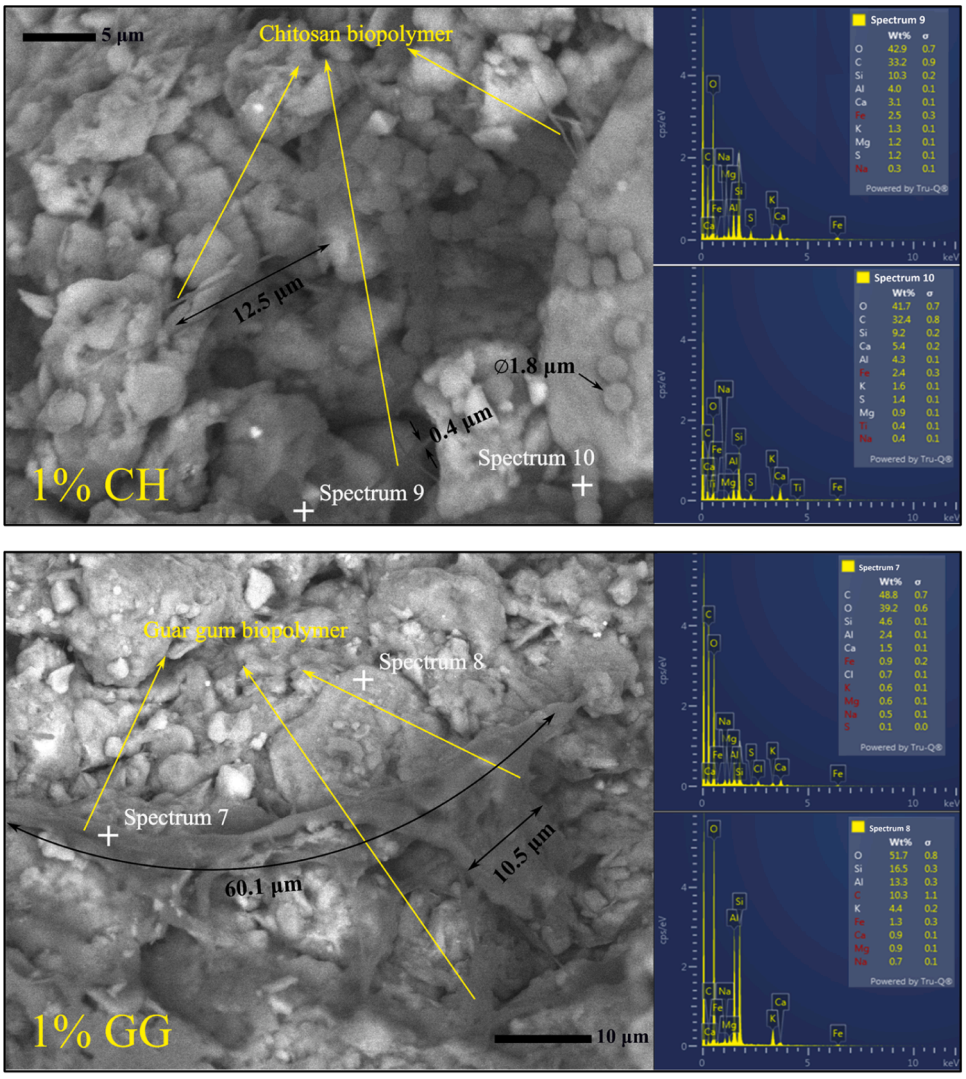

Fig. 13. (*continued*).

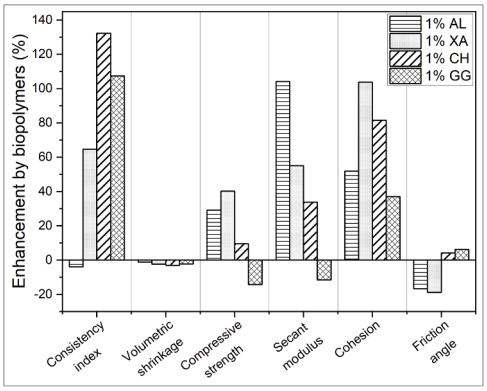

Fig. 14. Effect of different biopolymers on the geotechnical properties of dredged sediment.

reduction in the friction angle, indicating that while XA strengthens interparticle bonding, it may reduce friction through the formation of lubricating gel films as demonstrated in SEM imaging. In terms of shear strength, CH exhibits the best performance with significantly enhancing cohesion while also slightly increased the friction angle of the sediment.

The combined SEM, UCS, and direct shear results clearly show that biopolymer treatment fundamentally changes the soil microstructure and consequently, its overall mechanical behavior. The untreated sediment showed low compressive and shear strengths, aligning with SEM images displaying loosely packed grains with minimal interparticle bonds. Conversely, adding biopolymers introduced distinct binding mechanisms, as verified by the micrographs and EDS spectra. AL formed bridge-like, pore-filling films that increased cohesion and compressive strength, though its smooth surfaces limited gains in frictional resistance. XA developed fibrous, ribbon-like bridges that enabled efficient load transfer and strong interlocking, explaining its high UCS and improved shear resistance. CH created granular clusters that spot-welded particles and bridge-like formations, which moderately raised compressive strength while enhancing roughness and interlocking, which yielded notable shear strength gains. In contrast, GG formed wide gel-like films that promoted adhesion but lacked firm anchorage to the mineral skeleton, resulting in modest shear strength improvement and lower compressive strength.

Overall, the mechanical performance can be directly explained by the type and effectiveness of the polymer-soil bonds observed under SEM. Fibrous and continuous morphologies (XA, AL) produced stronger and more ductile responses under compression, while granular or rough surface morphologies (CH) were more effective in enhancing shear resistance. These findings confirm that the macroscopic strength of biopolymer-treated soils is governed not only by the amount of polymer

added but also by the specific microstructural bonding mechanism it introduces.

The current study compared the performance of four types of biopolymers in stabilizing dredged sediment. The results of this study can be used to select the appropriate biopolymer for stabilization of dredged sediment to be used for development of methodology for field-scale stabilization. The current study investigated the early strength enhancement using undrained shear strength estimation and consistency index calculation, while the mid-term behavior was studied by direct shear test and UCS after 28 days of curing.

5. Conclusion

Dredged marine sediments were treated with four types of biopolymers to investigate the potential stabilization enhancement in consistency, mechanical properties, and microstructural analysis of sediment. The findings of this study lead to the following conclusions:

- Incorporating 1 wt % biopolymers improved the mechanical properties of the dredged sediment, with varying levels of effectiveness depending on the biopolymer type. Therefore, biopolymers can be employed as sustainable bio-binders for dredged sediment stabilization, offering significant environmental benefits.
- The liquid limit and consistency of sediment increased significantly with biopolymers (except AL), which is a crucial improvement in dredged marine sediment that is characterized by high water content. Incorporating 1 wt % XA, CH, and GG increased the consistency index of the dredged sediment by 64 %, 132 %, and 107 %, respectively.
- Biopolymers slightly decreased the volumetric shrinkage of the sediment; however, this effect is minor.
- UCS of the sediment was enhanced by the addition of biopolymers, with the greatest improvement obtained in the XA-treated sample, which exhibited a 40 % increase in strength after 28 days of curing.
- Direct shear tests revealed that biopolymers significantly increased the cohesion of the sediment from 27 kPa to 41, 55, 49, and 37 kPa for sediment treated with AL, XA, CH, and GG, respectively. However, their effect on the friction angle varied: while AL and XA reduced the friction angle by 4°, CH- and GG-treated samples exhibited an increase in the sediment's friction angle by 1°.
- SEM observations and EDS analyses confirmed that biopolymers alter soil structure through different bonding mechanisms. These findings confirm that the strength enhancement of biopolymer-treated soils is governed not only by the amount of polymer added but also by the specific microstructural bonding mechanism it introduces.

CRediT authorship contribution statement

Yaser Ghafoori: Writing – original draft, Visualization, Software, Methodology, Investigation, Funding acquisition, Formal analysis, Data curation, Conceptualization. **Pooria Ghadir:** Writing – review & editing, Validation, Methodology, Investigation. **Sabina Dolenec:** Writing – review & editing, Supervision, Resources, Funding acquisition, Data curation. **Stanislav Lenart:** Writing – review & editing, Resources, Project administration, Investigation, Funding acquisition, Conceptualization.

Declaration of competing interest

The authors declare that they have no known competing financial interests or personal relationships that could have appeared to influence the work reported in this paper.

Acknowledgements

The authors acknowledge the project Bio4S, financially supported by the Slovenian Research and Innovation Agency through the Development funding pillar (RSF). The authors also acknowledge the financial support of the Slovenian Research and Innovation Agency (ARIS) through the program group P2–0273 Building structures and materials and project L2–60150: Bio- and alkali- activated stabilization of dredged marine sediments for inland, shore and offshore construction purposes (BAST).

Data availability

Data will be made available on request.

References

[1] G. Thomas, C. Isabelle, H. Frederic, P. Catherine, B. Marie-Anne, Demonstrating the influence of sediment source in dredged sediment recovery for brick and tile production, Resour. Conserv. Recycl. 171 (2021) 105653, https://doi.org/10.1016/j.resconrec.2021.105653.
[2] M. Bortali, M. Rabouli, M. Yessari, A. Hajjaji, Assessment of harbor sediment contamination for a path to valorize dredged material, Arab. J. Chem. 16 (2023) 105208, https://doi.org/10.1016/j.arabjc.2023.105208.
[3] C.-F. Chen, Y.C. Lim, Y.-R. Ju, F.P.J.B. Albarico, C.-W. Chen, C.-D. Dong, A novel pollution index to assess the metal bioavailability and ecological risks in sediments, Mar. Pollut. Bull. 191 (2023) 114926, https://doi.org/10.1016/j.marpolbul.2023.114926.
[4] R. Snellings, Ö. Cizer, L. Horckmans, P.T. Durdziński, P. Dierckx, P. Nielsen, K. Van Balen, L. Vandewalle, Properties and pozzolanic reactivity of flash calcined dredging sediments, Appl. Clay. Sci. 129 (2016) 35–39, https://doi.org/10.1016/j.clay.2016.04.019.
[5] P. Crocetti, J. González-Camejo, K. Li, A. Foglia, A.L. Eusebi, F. Fatone, An overview of operations and processes for circular management of dredged sediments, Waste Manag. 146 (2022) 20–35, https://doi.org/10.1016/j.wasman.2022.04.040.
[6] F.A. Jahromi, B. Keshavarzi, F. Moore, S. Abbasi, R. Busquets, P.S. Hooda, N. Jaafarzadeh, Source and risk assessment of heavy metals and microplastics in bivalves and coastal sediments of the Northern Persian Gulf, Hormogzan Province, Environ. Res. 196 (2021) 110963, https://doi.org/10.1016/j.envres.2021.110963.
[7] D. Sundary, R.P. Munirwan, N. Al-Huda, M.Sungkar Munirwansyah, R.P. Jaya, Shear strength performance of dredged sediment soil stabilized with lime, Phys. Chem. Earth, Parts A/B/C 128 (2022) 103299, https://doi.org/10.1016/j.pce.2022.103299.
[8] Supakij Nontananandh, Nattapas Khumsuprom, Thanet Thongdetsri, Sukit Youdee, Apiniti Jotisankasa, Susit Chaiprakaikeow, Shinya Inazumi, Cement stabilization of dredged sediments from drainage canals: effect on physico-chemical properties, GEOMATE J. 27 (2024) 143–150. https://geomatejournal.com/geomate/article/view/4863.
[9] A.M. Abdelbaset, D. Katunský, M. Zeleňáková, M.H. El-Feky, Mechanical properties stabilization of low plasticity Kaolin soil using fly ash and hydrated lime, Case Stud. Construct. Mater. 21 (2024) e03662, https://doi.org/10.1016/j.cscm.2024.e03662.
[10] C. Li, X.Z. Gong, S.P. Cui, Z.H. Wang, Y. Zheng, B.C. Chi, CO2 Emissions due to cement manufacture, Energy, Environ. Biolog. Mater., Trans. Tech. Public. Ltd (2011) 181–187, https://doi.org/10.4028/www.scientific.net/MSF.685.181.
[11] A. Sagastume Gutiérrez, J. Van Caneghem, J.B. Cogollos Martínez, C. Vandecasteele, Evaluation of the environmental performance of lime production in Cuba, J. Clean. Prod. 31 (2012) 126–136, https://doi.org/10.1016/j.jclepro.2012.02.035.
[12] M. Malarski, P. Wichowski, J. Czajkowska, Heavy metals in fly ash as a factor limiting its use in fertilizing composts, Water. (Basel) (2023) 15, https://doi.org/10.3390/w15122247.
[13] K.M.N.S. Wani, B.A. Mir, Influence of microbial geo-technology in the stabilization of dredged soils, International Journal of Geotechnical Engineering 15 (2021) 235–244, https://doi.org/10.1080/19386362.2019.1643099.
[14] V. Ivanov, J. Chu, Applications of microorganisms to geotechnical engineering for bioclogging and biocementation of soil in situ, Rev. Environ. Sci. Biotechnol. 7 (2008) 139–153, https://doi.org/10.1007/s11157-007-9126-3.
[15] K.M.N.S. Wani, B.A. Mir, A laboratory-scale study on the bio-cementation potential of distinct river sediments infused with microbes, Transportat. Infrastruct. Geotechnol. 8 (2021) 162–185, https://doi.org/10.1007/s40515-020-00131-w.
[16] T. Terui, T. Motohashi, S. Sasahara, S. Inazumi, Development and application of geothermally derived silica grout for carbon-neutral soil stabilization, Case Stud. Construct. Mater. 22 (2025) e04297, https://doi.org/10.1016/j.cscm.2025.e04297.
[17] R. Showkat, B.A. Mir, K.M.N.S. Wani, Experimental investigation on reuse of dredged soils improved using waste rubber tyre powder (WRTP) and cement as admixtures, Geomechan. Geoeng. 19 (2024) 950–964, https://doi.org/10.1080/17486025.2024.2334265.

[18] M. Nasrollahzadeh, M. Sajjadi, S. Iravani, R.S. Varma, Starch, cellulose, pectin, gum, alginate, chitin and chitosan derived (nano)materials for sustainable water treatment: a review, Carbohydr. Polym. 251 (2021) 116986, https://doi.org/10.1016/j.carbpol.2020.116986.
[19] J. Liu, W. Che, X. Lan, M. Hu, M. Qi, Z. Song, M. Sun, M. Jing, W. Qian, C. Qi, Performance and mechanism of a novel biopolymer binder for clayey soil stabilization: mechanical properties and microstructure characteristics, Transport. Geotechn. 42 (2023) 101044, https://doi.org/10.1016/j.trgeo.2023.101044.
[20] M.K. Ayeldeen, A.M. Negm, M.A. El Sawwaf, Evaluating the physical characteristics of biopolymer/soil mixtures, Arabian J. Geosci. 9 (2016) 371, https://doi.org/10.1007/s12517-016-2366-1.
[21] M. Hamza, Z. Nie, M. Aziz, N. Ijaz, O. Akram, C. Fang, M.U. Ghani, Z. Ijaz, S. Noshin, M.F. Madni, Geotechnical behavior of high-plastic clays treated with biopolymer: macro–micro-study, Environ. Earth. Sci. 82 (2023) 91, https://doi.org/10.1007/s12665-023-10760-2.
[22] M. Lee, Y.-M. Kwon, D.-Y. Park, I. Chang, G.-C. Cho, Durability and strength degradation of xanthan gum based biopolymer treated soil subjected to severe weathering cycles, Sci. Rep. 12 (2022) 19453, https://doi.org/10.1038/s41598-022-23823-4.
[23] F. Ren, H. Ding, B. Dong, X. Qian, J. Liu, J. Tan, Study on the improvement of soil properties using hydrophilic-hydrophobic biopolymer crosslinking, Constr. Build. Mater. 415 (2024) 135101, https://doi.org/10.1016/j.conbuildmat.2024.135101.
[24] J. Zhang, Z. Meng, T. Jiang, S. Wang, J. Zhao, X. Zhao, Experimental study on the shear strength of silt treated by Xanthan gum during the wetting process, Appl. Sci. 12 (2022), https://doi.org/10.3390/app12126053.
[25] E.R. Sujatha, S. Atchaya, A. Sivasaran, R.S. Keerdthe, Enhancing the geotechnical properties of soil using xanthan gum—An eco-friendly alternative to traditional stabilizers, Bulletin Eng. Geol. Environ. 80 (2021) 1157–1167, https://doi.org/10.1007/s10064-020-02010-7.
[26] I. Chang, Y.-M. Kwon, J. Im, G.-C. Cho, Soil consistency and interparticle characteristics of xanthan gum biopolymer–containing soils with pore-fluid variation, Canadian Geotechn. J. 56 (2019) 1206–1213, https://doi.org/10.1139/cgj-2018-0254.
[27] F. Abbasi, A. Janalizadeh Choobbasti, K. Roushan, Advanced stabilization of clayey sand using xanthan gum: insights from multiscale evaluation and ultrasonic pulse velocity analysis, Results. Eng. 25 (2025) 104419, https://doi.org/10.1016/j.rineng.2025.104419.
[28] R. Wang, D.E.L. Ong, H. Sadighi, M. Goli, P. Xia, H. Fatehi, T. Yao, Optimizing soil stabilization with Chitosan: investigating acid concentration, temperature, and long-term strength, Polymers. (Basel) (2025) 17, https://doi.org/10.3390/polym17020151.
[29] N. Shariatmadari, M. Amiri Tasuji, P. Ghadir, A. Javadi, Experimental study on the effect of chitosan biopolymer on sandy soil stabilization, E3S Web Conf. 195 (2020) 6007, https://doi.org/10.1051/e3sconf/202019506007.
[30] M. Amiri Tasuji, P. Ghadir, A. Hosseini, A.A. Javadi, A. Habibnejad Korayem, N. Ranjbar, Experimental investigation of sandy soil stabilization using chitosan biopolymer, Transport. Geotechn. 46 (2024) 101266, https://doi.org/10.1016/j.trgeo.2024.101266.
[31] G. Kannan, E.R. Sujatha, Crustacean polysaccharides for the geotechnical enhancement of organic silt: a clean and green alternative, Carbohydr. Polym. 299 (2023) 120227, https://doi.org/10.1016/j.carbpol.2022.120227.
[32] M. Azimi, A. Soltani, M. Mirzababaei, M.B. Jaksa, N. Ashwath, Biopolymer stabilization of clayey soil, J. Rock Mechan. Geotechn. Eng. 16 (2024) 2801–2812, https://doi.org/10.1016/j.jrmge.2023.12.020.
[33] N. Hataf, P. Ghadir, N. Ranjbar, Investigation of soil stabilization using chitosan biopolymer, J. Clean. Prod. 170 (2018) 1493–1500, https://doi.org/10.1016/j.jclepro.2017.09.256.
[34] X. Rong, S. Deng, B. Liang, J. Zhuang, Y. Yu, Z. Wu, Mechanical behavior and strengthening mechanism of loess stabilized with xanthan gum and guar gum biopolymers, Mater. Res. Express. 11 (2024) 105305, https://doi.org/10.1088/2053-1591/ad832c.
[35] X. Du, H. Tian, X. Kang, Z. Sun, X. Zhao, Y. Ren, Strength and water retention behavior of loess stabilized with guar gum and fiber under dry and wet cycles, Sci. Rep. 15 (2025) 11410, https://doi.org/10.1038/s41598-025-96390-z.
[36] Y. Ji, N. Zheng, Q. An, S. Wang, S. Sun, X. Li, C. Chen, S. Sun, Y. Jiang, Enhanced immobilization of cadmium and lead in contaminated soil using calcium alginate-modified HAP biochar: improvements in soil health and microbial diversity, Environ. Pollut. 357 (2024) 124445, https://doi.org/10.1016/j.envpol.2024.124445.
[37] Q. Feng, M. Chen, P. Wu, X. Zhang, S. Wang, Z. Yu, B. Wang, Calcium alginate-biochar composite as a novel amendment for the retention and slow-release of nutrients in karst soil, Soil. Tillage Res. 223 (2022) 105495, https://doi.org/10.1016/j.still.2022.105495.
[38] S. Houben, L.M. Pitet, Ionic crosslinking strategies for poly(acrylamide) /alginate hybrid hydrogels, React. Funct. Polym. 191 (2023) 105676, https://doi.org/10.1016/j.reactfunctpolym.2023.105676.
[39] S. Liu, K. Du, K. Wen, C. Armwood-Gordon, Y. Li, I. Navarro, L. Li, Stabilization of expansive clayey soil through hydrogel for mechanical improvements, Int. J. Civil Eng. 21 (2023) 1423–1431, https://doi.org/10.1007/s40999-023-00835-3.
[40] A. Bakhshizadeh, N. Khayat, S. Horpibulsuk, Surface stabilization of clay using sodium alginate, Case Stud. Construct. Mater. 16 (2022) e01006, https://doi.org/10.1016/j.cscm.2022.e01006.
[41] N. Rogan Šmuc, M. Dolenec, S. Kramar, A. Mladenović, Heavy metal signature and environmental assessment of nearshore sediments: port of Koper (Northern Adriatic Sea), Geosciences. (Basel) 8 (2018), https://doi.org/10.3390/geosciences8110398.
[42] ISO, Geotechnical investigation and testing - laboratory testing of soil - part 4: determination of particle size distribution (ISO 17892-4:2016), Int. Organiz. Standardiz. (ISO) (2016).
[43] ASTM International, ASTM D698-12: standard test methods for laboratory compaction characteristics of soil using standard effort, 2021.
[44] ISO, Geotechnical investigation and testing - laboratory testing of soil -part 12: determination of liquid and plastic limits (ISO 17892-12:2018), Int. Organiz. Standardiz. (ISO) (2018).
[45] S. Hansbo, New approach to the determination of the shear strength of clay by the fall-cone test, 1957.
[46] ISO, ISO 17892-6:2017 geotechnical investigation and testing – Laboratory testing of soil – part 6. Fall cone test, Int. Organiz. Standardiz. (ISO) (2017).
[47] M. Asha, H.B. Nagaraj, S. Muguda, Shrinkage limit determination of soils using hydrophobic compounds, Geotech. Geol. Eng. (Dordr) 43 (2025) 214, https://doi.org/10.1007/s10706-025-03162-7.
[48] ISO, Geotechnical investigation and testing - laboratory testing of soil -part 7: unconfined compressive test (ISO 17892-7:2017), Int. Organiz. Standardiz. (ISO) (2017).
[49] ELE International, Digital direct/residual shear apparatus complete with lever loading assembly, (2023).
[50] ISO, Geotechnical investigation and testing - laboratory testing of soil -part 10: direct shear tests (ISO 17892-10:2019), Int. Organiz. Standardiz. (ISO) (2019).
[51] N. Bayliss, B.V.K.J. Schmidt, Hydrophilic polymers: current trends and visions for the future, Prog. Polym. Sci. 147 (2023) 101753, https://doi.org/10.1016/j.progpolymsci.2023.101753.
[52] A. Soldo, M. Miletić, M.L. Auad, Biopolymers as a sustainable solution for the enhancement of soil mechanical properties, Sci. Rep. 10 (2020) 267, https://doi.org/10.1038/s41598-019-57135-x.
[53] R.M. Rasheed, A.A.B. Moghal, S.S.R. Jannepally, A.U. Rehman, B.C.S. Chittoori, Shrinkage and consolidation characteristics of Chitosan-amended soft soil—A sustainable alternate landfill liner material, Buildings 13 (2023), https://doi.org/10.3390/buildings13092230.
[54] J. Gu, J. Ni, S. Liu, Y. Chen, Shear strength of biopolymer amended soil under freeze-thaw cycles: experimental investigation and DEM modeling, Eng. Geol. 353 (2025) 108108, https://doi.org/10.1016/j.enggeo.2025.108108.
[55] A. Soldo, M. Miletić, Study on shear strength of Xanthan gum-amended soil, Sustainability. 11 (2019), https://doi.org/10.3390/su11216142.